



1 Uncovering a Key Predictors for Enhancing Daily Streamflow Simulation Using 2 Machine Learning

3 Arash Aghakhani^{a,b,*}, David E. Robertson^a, Valentijn R.N. Pauwels^b

4 ^a Commonwealth Scientific and Industrial Research Organisation (CSIRO), Clayton 3168, Australia

5 ^b Department of Civil Engineering, Monash University, Clayton, VIC 3800, Australia

6 Correspondence: Arash Aghakhani, arash.aghakhani86@gmail.com

7 Abstract

8 The sequence of droughts and wetter periods in Australia poses challenges for long-term hydrologic
9 modelling. This paper develops a novel machine learning-based approach to uncover key predictors that
10 improve daily streamflow predictions during and after the Millennium drought (1997 to 2009) in 39
11 gauged sub-catchments in Western Victoria, Australia.

12 For this purpose, a hybrid approach is adopted, combining simulations from the GR4J hydrological
13 model with physical data as forcing (predictors) for multiple ML algorithms to identify the key
14 predictors for improving streamflow prediction. GR4J is a widely used operational hydrological model
15 in Australia. ML models including predictors representing long-term runoff coefficient and short-term
16 runoff and rainfall showed the greatest improvement in streamflow predictions, particularly for low
17 flows. This suggests that GR4J has limited ability to capture short/long-term persistence and therefore
18 model enhancement should focus on these shortcomings. All ML algorithms resulted in improved
19 streamflow prediction, with Multilayer Perceptron (MLP) consistently yielding the highest Nash
20 Sutcliffe Efficiency, and Random Forest showing the strongest improvement in terms of low-flow
21 prediction. Long-term runoff coefficient and machine learning were most effective in catchments with
22 lower long-term runoff coefficients. Overall, this study provides insights for water resources
23 management in drought-prone regions, highlighting the key predictors in the combination of ML and
24 hydrological modelling to improve streamflow predictions during and after droughts.



25 Keywords: Machine learning, streamflow prediction, Millennium drought, Climate change,
26 Hydrological model, long/short-term runoff coefficient

27 **1 Introduction**

28 Climate change is projected to increase the frequency and severity of droughts in many parts of the
29 world due to reductions in rainfall (Fowler et al., 2022). Analysis of historical multi-year droughts can
30 therefore provide insights and understanding of hydrological responses likely to be observed under
31 future climate changes (Fowler et al., 2022). Australia's Millennium drought (1997 to 2009) serves as a
32 noteworthy example (Van Dijk et al., 2013). During the Millennium drought, a substantial portion of the
33 southern part of Australia faced an extended period of dry conditions. The impact was particularly
34 severe in densely populated areas of Southeastern and Southwestern Australia (Bureau of Meteorology,
35 2024) (Wallis et al., 2011) (Southwest Victoria alliance-Advocacy Priorities 2021/22, 2024) (Primary
36 Production Landscapes of Victoria - Northwest Victoria, (2024)). During the Millennium drought, soil
37 drying and declining water tables harmed flora and fauna, leading to more wildfires and dust storms
38 (Heberger, 2012). The sheep population during the Millennium drought in Australia declined by half
39 (Heberger, 2012). Water shortages due to the Millennium drought led to decreased water allocations for
40 irrigation, imposed water restrictions in urban areas, and prompted considerable investments in
41 infrastructure, such as the construction of desalination plants and pipeline installation (Van Dijk et al.,
42 2013).

43 Southwestern Victoria, as part of southeastern Australia severely impacted during the Millennium
44 Drought, reflects the nation's broader struggle with prolonged dry conditions. During the Millennium
45 drought, alterations, or shifts (Saft et al., 2015), in rainfall-runoff relationships were observed in
46 numerous Victorian catchments but were absent in others (Fowler et al., 2022). These shifts in rainfall-
47 runoff relationships are a form of hydrologic non-stationary. Non-stationarity in hydrology refers to the
48 phenomenon where the statistical properties of hydrological processes, such as rainfall patterns and
49 runoff relationships, change over time. In other words, the influence of forcing variables in one period
50 will differ from those experienced in a separate period (Slater et al., 2021). During the Millennium



51 drought reductions in streamflow were larger than initially anticipated based on the observed rainfall
52 reductions (van Rensch et al., 2023). The physical mechanisms behind these shifts are not well
53 understood (Fowler et al., 2022). According to Peterson et al. (2021), the transitions towards reduced
54 streamflow can exhibit remarkable persistence, as certain watersheds appear to maintain a changed state
55 even after returning to nearly average climate conditions. In these persisting cases, a year of typical
56 rainfall now results in lower streamflow compared to pre-drought levels.

57 Streamflow prediction is challenging due to its high complexity, non-stationarity, and non-linearity of
58 hydrological processes (Yaseen et al., 2015). Many Process-Based (PB) hydrological models have been
59 developed for streamflow prediction. However, due to the uncertainties in the formulation and
60 parameterisation of the physical processes, and also the errors in the forcings and validation data, these
61 models exhibit limited capability in capturing the non-stationary in hydrological datasets (Cheng et al.,
62 2020). Conceptual hydrological models are widely used for climate change impact analyses due to their
63 higher computational efficiency, facilitating rapid assessments across multiple catchments and for long-
64 term simulations (Zheng et al., 2024) However, their simplified representation of the physical processes
65 potentially overlooks the ways within-catchment hydrological processes could intensify or alleviate
66 changes in runoff generation under a changing climate (Robertson et al., 2023). Since the physical
67 mechanisms behind the shifts in rainfall-runoff relationships are not well understood, such shifts in
68 response to extended drought are challenging to predict. Furthermore, it is widely accepted that the use
69 of hydrological models for prediction in changing conditions remains a significant concern in hydrology
70 (Blöschl et al., 2019).

71 Model validation against a diverse range of conditions is a crucial step in building robust models
72 (Fowler et al., 2022). Hydrological models developed and calibrated based on pre-drought data are not
73 capable of properly predicting the streamflow during the drought (Chiew et al., 2014). Fowler et al.
74 (2021) studied the performance of the GR4J hydrological model in Victoria's catchments for the
75 Millennium drought and suggested that limitations in conceptual hydrological models capabilities to
76 project runoff under a drying climate might be due to implicit upper limits on the soil moisture deficit.
77 Chiew et al. (2014) modelled 20 catchments in South-Eastern Australia, using the SIMHYD model, and



78 found that pre-drought optimised parameter values resulted in very poor Millennium drought daily
79 streamflow simulations. They stated that this poor performance is related to the hydrologic non-
80 stationarity.

81 Machine learning models have proven highly effective in modelling natural systems because they do
82 not make prior assumptions on the form of equations describing physical processes that are necessary
83 in traditional models (Reis et al., 2021). Over the past two decades, there has been substantial
84 advancement in the application of artificial intelligence and machine learning (ML) methods to predict
85 non-linear hydrological responses (Pradhan et al., 2020), and generate valuable insights into the
86 physical mechanisms behind hydrologic non-stationarities (Hao and Bai, 2023). The popularity of ML
87 models for streamflow prediction is related to their relative ease of application, competitive
88 computational performance and prediction accuracy (Pham et al., 2021). Machine learning methods are
89 also less rigid in assumptions used to characterize the probability distribution of model errors than other
90 methods, including statistical modelling. PB and ML approaches can complement each other with
91 respect to their strengths and limitations. Hydrologic processes that preserve the mass and energy
92 balance can be captured by a PB model, while other processes not incorporated in a PB model can be
93 covered by the data-driven ML algorithm. Thus, an effective strategy is a hybrid combination of both
94 approaches to improve hydrologic simulation (Konapala et al., 2020).

95 In ML, computers learn from data patterns to make predictions without the need for code development
96 by the user. Input data (predictors) are used to predict output variables. Various machine learning
97 methodologies have been employed in hydrological research for predicting streamflow, (Deo and Şahin,
98 2016; Petty and Dhingra, 2018; Yaseen et al., 2016). These approaches are based on diverse techniques
99 such as Linear Regression, Multiple Linear Regression (MLR), Ridge regression, Gradient Boosting
100 and its variants, neural networks (NN), specifically Multilayer Perceptron (MLP), and long short-term
101 memory (LSTM), support vector machines (SVM), Decision tree, and Random Forest (RF), among
102 others. Recent research indicates that ML models exhibit robustness and efficiency, often surpassing
103 the performance of traditional hydrological models, including both conceptual and physically-based
104 approaches, (Akusok et al., 2015; Rozos et al., 2022; Worland et al., 2018).



105 Numerous reviews of the use of artificial intelligence and machine learning for hydrological
106 applications have been published (Ng et al., 2023; Mohammadi, 2021; Yaseen et al., 2015). These
107 reviews have all concluded that ML methods are highly suited to runoff prediction and forecasting
108 applications due to their ability to represent non-linear and highly complex relationships between
109 prediction variables and their predictors, and integrate a large range of complex and noisy datasets
110 published (Ng et al., 2023; Mohammadi, 2021; Yaseen et al., 2015)

111 However, no standardised guidance exists for selecting ML methods to achieve optimal simulation
112 accuracy (Hao and Bai, 2023) and choosing a single ML algorithm with high predictive accuracy is
113 challenging, because algorithm performance depends on the specific datasets used and problem being
114 addressed (Hao and Bai, 2023; Worland et al., 2018). A number of studies have reported varying
115 outcomes regarding the comparison of the performance of different algorithms (Section 2.2.2.8). The
116 algorithm is not the only factor of influence on the prediction results, the quality and quantity of the
117 input data (predictors) has been shown to have a strong impact as well.

118 Moosavi et al. (2022) highlighted that the volume of input data (predictors) had stronger impact on the
119 prediction accuracy in comparison to the model type. The lack of adequate predictor selection, or the
120 use of an excessive number of predictors, affects the precision and stability of prediction models. This
121 situation also necessitates a substantial amount of memory and computational resources for training and
122 validation procedures (Reis et al., 2021). Therefore, identifying a suitable set of predictors is a crucial
123 step in the ML modelling process. ML algorithms may produce less accurate and less interpretable
124 results when working with insufficient data, or with data containing irrelevant or redundant information.
125 In hydrologic problems, nonlinear approaches are often preferred for determining the type of model
126 inputs, given the demonstrated highly non-linear nature of the input–output relationships (Lima et al.,
127 2016).

128 Published studies have primarily focused on enhancing streamflow forecasting at the sub-catchment
129 scale through machine learning, rather than finding the predictors that lead to the greatest improvement
130 in the performance of predictions across a range of catchments. Additionally, there is a literature gap on
131 how machine learning can be used to improve hydrological models and to identify potential



132 enhancements that could be globally applicable. Therefore, in this study, ML is employed using a
133 combination of hydrological model outputs and physical data as predictors to investigate possible
134 improvements in prediction performance and identify components missing in the hydrological model
135 conceptualisation. For this purpose, GR4J, a simple yet efficient hydrological model (Arsenault et al.,
136 2019), appropriate for a range of climate conditions and commonly used in Australia (Stephens et al.,
137 2019) is used in this study.

138 The objectives of this study are: (1) to explore the effectiveness of using a combination of GR4J and
139 physical data as predictors for machine learning algorithms for streamflow prediction in Western
140 Victoria, Australia, during the drought and the post-drought periods, based on pre-drought calibration,
141 and (2) to reveal the catchment data that are overlooked or are too uncertain for the employed
142 hydrological model structure or configuration. This can be achieved by identifying the predictors with
143 a significant impact on the improvement of the model results, incorporating them as essential physical
144 parameters in the conceptual hydrological model, or by making alterations to the structure of the
145 hydrological model.

146 The paper is structured as follows: Section 2 describes the case study area and the methodology used in
147 this study. Section 3 presents results and discussion of the performance of hydrological model and
148 proposed ML models, followed by section 4 that summarises the key findings and conclusions from the
149 paper.



150 **2 Materials and methods**

151 **2.1 Case study**

152 For this case study we use streamflow data for 39 gauged sub-catchments of 9 major catchments in
153 western Victoria, Australia. This region depends significantly on agriculture, with approximately 81%
154 of the land use having been developed for agricultural uses (Wallis et al., 2011), and plays a vital role
155 in Australia's agricultural and forestry sectors. It contributes significantly to the nation's dairy
156 production generating 2.3 billion Australian dollars, or 27% of the total national value, annually. In
157 addition, it covers 17% of Australia's forest plantations (Southwest Victoria alliance-Advocacy
158 Priorities 2021/22, 2024). Northwestern Victoria contains 40% of Victoria's dryland agriculture
159 focusing mainly used for cereal cropping. Another significant land use in this area is grazing and
160 production from native vegetation, accounting for 13% of Victoria land area (Primary Production
161 Landscapes of Victoria - Northwest Victoria, 2024). This region has been chosen due to the notable
162 influence of the Millennium drought on the streamflow and its importance on Victoria's economy.

163 Figure 1 shows an overview of the study area. The study sub-catchment range in size from 4.5 km² to
164 approximately 2,677 km². The majority of the river runoff occurs during the austral winter and spring,
165 primarily attributed to rainfall. The details of the sub-catchments and stream gauge stations can be found
166 in Appendix (Table A. 1 and Figure A. 1). Streamflow data were extracted from the Bureau of
167 Meteorology (BoM) Hydrologic Reference Stations (Hydrologic Reference Stations, 2024).
168 Streamflow data are quality controlled using the quality flags provided, removing observations
169 characterised as estimates, poor or unknown quality (Zhang et al., 2016). Catchment average forcing
170 data, specific are derived by taking area-weighted averages of the Australian Gridded Climate Data
171 (Jones et al., 2009), rainfall and AWRA potential evapotranspiration (Frost, 2018).

172

173



174 2.2 Methods

175 To quantify the impact of the Millennium drought, changes in the mean daily rainfall and mean daily
 176 streamflow were calculated using the following equations:

177

$$Rainfall\ change = \frac{rainfall_{p2} - rainfall_{p1}}{rainfall_{p1}} \times 100 \quad Eq. 1$$

178

$$Streamflow\ change = \frac{Streamflow_{p2} - Streamflow_{p1}}{Streamflow_{p1}} \times 100 \quad Eq. 2$$

179

180 Where:

181 $Rainfall_{p1}$: mean daily rainfall in the period from 1988-01-01 to 1996-12-31 (pre-drought)

182 $Rainfall_{p2}$: mean daily rainfall in the period from 1997-01-01 to 2018-12-31 (drought and post-drought)

183 $Streamflow_{p1}$: mean daily Streamflow in the period from 1988-01-01 to 1996-12-31 (pre-drought)

184 $Streamflow_{p2}$: mean daily Streamflow in the period from 1997-01-01 to 2018-12-31 (drought and post-
 185 drought)

186 Since this study investigates the integration of results from a conceptual hydrological model with ML
 187 algorithms, the remainder of this section focuses on a general discussion on both the conceptual
 188 hydrological model and ML algorithms. Subsequently, the explanation of the proposed models is
 189 provided for comprehensive understanding of the combined approach used in this research.

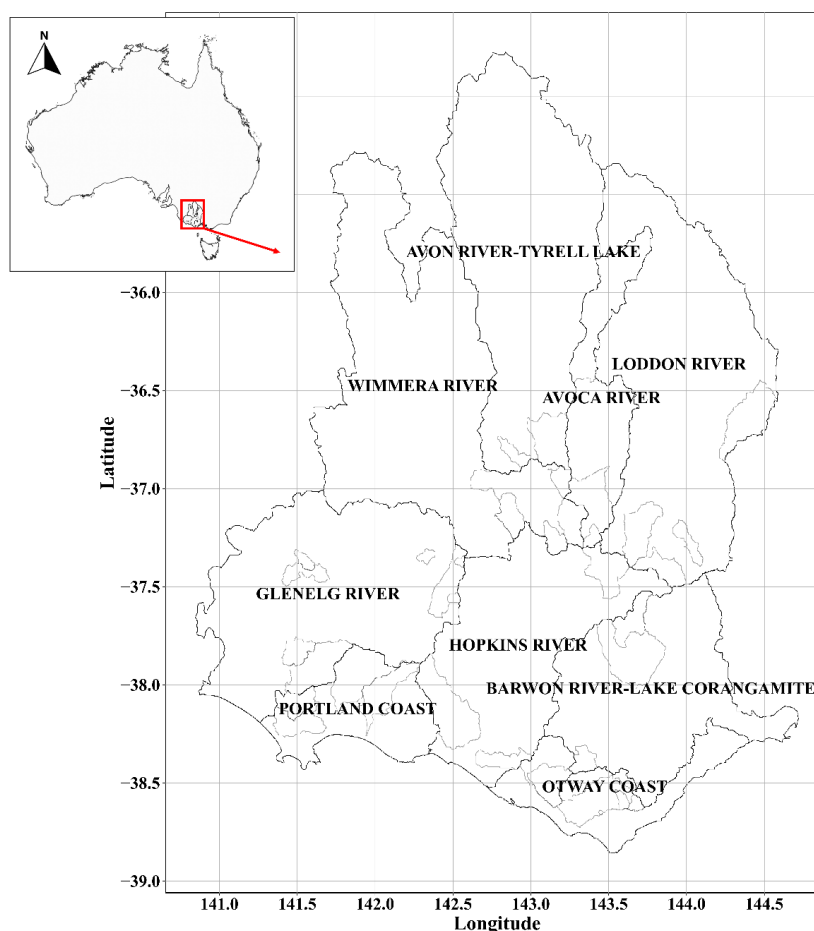
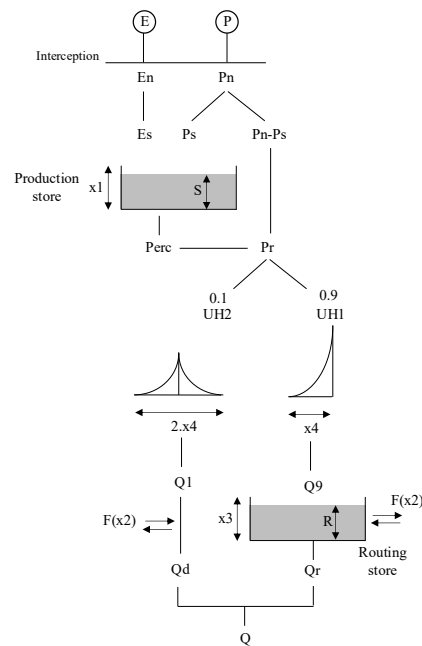


Figure 1. Overview of the catchments and sub-catchments used in this study (projection: EPSG:4326).

2.2.1 Hydrological models

The hydrological model used as a predictor for the ML models in this study is GR4J (Perrin et al., 2003).

A schematic of GR4J is shown in Figure 2. This model is a four-parameter model that has been demonstrated to perform well in Australia. Model calibration and simulation was undertaken using the SWIFT2 (Short-term Water Information and Forecasting Tools) software (Perraud et al., 2015). The GR4J model parameters {X1, X2, X3 and X4} were calibrated by maximising the Nash-Sutcliffe Efficiency (NSE) using the Shuffled Complex Evolution (Aryal et al., 2020; Duan et al., 1994; Perrin et al., 2003).



200

201

Figure 2 Diagram of GR4J hydrological model, with parameters derived from (Perrin et al., 2003)

202

2.2.2 Machine learning algorithms

203

Various machine learning algorithms are assessed in this study, namely Linear Regression, Ridge Regression, Support Vector Regression (SVR), Decision Tree, Random Forest, Gradient Boosting, and MLP. While all algorithms improved streamflow prediction accuracy, only the results of Random Forest, Gradient Boosting, and MLP are presented as they produced the best performing predictions (Ayzel et al., 2021; Lees et al., 2021; Rozos et al., 2022).

208

2.2.2.1 Random Forest regression

209

Random Forest regression generates predictions from an ensemble of regression relationships fitted over subsets of the predictor space that are defined using decision trees. This algorithm enhances the stability of decision trees by randomly sampling from the training data with replacement and aggregating the results. The combination of diverse trees also reduces prediction errors. This ensemble method is referred to as Random Forest, given that numerous trees are grown in a 'random' manner (Li et al., 2020). Random Forest is a simple and fast algorithm and one of the most powerful statistical

214



215 learning methods. It has the ability to work with very large datasets and is widely used in hydrological
216 applications (Roy and Larocque, 2012; Szczepanek, 2022). Random Forest avoids assuming a global
217 functional relationship and uses a local fitting approach through recursive partitioning. It exhibits
218 flexibility regarding the distributional assumptions of model residuals (Li et al., 2020). This algorithm
219 decreases variance by averaging decisions across diverse classifiers. Additionally, it diminishes bias
220 when individual classifiers are adequately complex for the given subset of features (Yeturu, 2020).
221 Random forest is considered in this study since many previous comparisons stated its remarkable
222 performance (Bentéjac et al., 2021) and its key advantage in avoiding overfitting issues through an
223 ensemble of permutations. Additionally, RF model evaluates the importance of predictor variables,
224 enhancing interpretability compared to methods like artificial neural networks (ANNs) and SVR
225 (Tongal and Booi, 2018)

226 2.2.2.2 Gradient Boosting

227 Gradient boosting algorithm is widely recognised as one of the most powerful algorithms (Wang et al.,
228 2022) which can fit complex nonlinear relationships (He et al., 2020). Gradient boosting iteratively
229 combines weak learners, which are slightly better than random, to form a suitable learner. This
230 technique is commonly used for regression tasks. The objective of gradient boosting, when applied to
231 a training dataset, is to minimise the expected value of a specified loss function to approximate the data
232 (Bentéjac et al., 2021). Gradient boosting algorithms are well-known for their ability to effectively
233 handle missing data and intricate relationships (Kumar et al., 2023). This method is commonly
234 employed with decision trees of a fixed size as the base learners. Boosted decision trees are widely
235 recognised as among the most effective prediction algorithms available today (Biau et al., 2019). In this
236 study, gradient boosting is applied as a method for addressing a regression problem.

237 2.2.2.3 MLP

238 Multilayer Perceptron (MLP) is the most popular type of neural network in hydrology, renowned for its
239 excellent performance in predicting streamflow (Boucher et al., 2020; Mohammadi et al., 2020;
240 Rahimzad et al., 2021). This algorithm is a feedforward artificial neural network, which consists of
241 interconnected nodes organised into three types of layers: input, hidden, and output. The input layer



242 transmits input values to the hidden layer without performing any operations on the input signal. The
243 hidden layer processes signals from the input layer nodes, transforming them into signals distributed to
244 all output nodes. The output nodes, in turn, further transform these signals into final outputs. This
245 architecture is particularly effective for addressing non-linear problems (Onyari and Ilunga, 2013). In
246 this study the MLP had 1 hidden layer and 100 neurons.

247 2.2.3 Model application

248 An overall schematic of the applied methodology is provided in Figure 3. Data were divided into
249 training and test periods that extended from January 1, 1988, through December 31, 1996, representing
250 the pre-drought period. Independent predictions were performed for the period January 1, 1997, through
251 December 31, 2018, covering the Millennium drought and post-drought periods. Calibration and
252 optimisation were conducted for the training and test periods only, and the subsequent simulation was
253 carried out for the prediction period.

254 In the implementation of the machine learning analysis, different combinations of various predictors
255 were considered in addition to the outcomes of the hydrological model. These predictors include
256 rainfall, potential evapotranspiration, short-term streamflow memory, short-term rainfall memory, and
257 long-term runoff coefficient. Short-term streamflow memory is characterised by the average streamflow
258 over the preceding two days. Similarly, short-term rainfall memory is characterised by the average
259 rainfall over the previous two days, offering a snapshot of recent precipitation patterns. The short-term
260 rainfall and streamflow are expected to provide insight into the hydrological responses lag. The long-
261 term runoff coefficient was derived by evaluating the ratio of cumulative runoff to cumulative rainfall
262 for a five-year window leading up to each date. The long-term runoff coefficient is assumed to be
263 associated with changes in catchment characteristics and particularly those related to surface-
264 groundwater interactions (Robertson et al., 2023).

265 Eight ML models were assessed through different combinations of predictors, as outlined in Figure 3.
266 For models 5 and model 6, an intentional effort was undertaken to account for the influence of long-
267 term runoff coefficient on the estimation of the fraction of the rainfall contributing to streamflow. This



268 is achieved by multiplying the derived ratio of the five-year streamflow to precipitation, with both the
269 rainfall and short-term rainfall memory components.

270 For each model, all ML algorithms listed in section 2.2.2 were trained using the SKlearn package in
271 python, using data for the period January 1, 1988, through December 31, 1996. The objective function
272 of all algorithms is squared error. The ML training process requires specification of training and testing
273 subsets. The division of the data into training and testing periods can have a material impact on the
274 fitted algorithm and its predictive performance. For this study, we adopted an 80:20 ratio of training to
275 testing periods. The ML model training process was repeated ten times, each time randomly allocating
276 data for the period January 1, 1988, through December 31, 1996 to the training and testing periods. All
277 ten of the fitted ML models were retained to form an ensemble.

278 The fitted ML models were then used to generate predictions for the period January 1, 1997, through
279 December 31, 2018. When the ML models are in predictive mode, the predictors representing long-term
280 and short-term streamflow memories can be derived from observations. Using streamflow observations,
281 the ML model's predictions are continually adjusted by the most recent observation, and predictions are
282 equivalent to lead-one forecasts forced by perfect rainfall forecasts. The process begins by initialising
283 the model with historical data. Then, the model predicts streamflow for the first day using the most
284 recent observations. After each prediction, the observed streamflow for that day is integrated into the
285 model as input for the following day prediction. This iterative process continues for the prediction of
286 the following days. This evaluation will inform limitations in the structure of the GR4J model and
287 identify processes, such as short-term or long-term memory, that may require improvement.
288 Additionally, if potential evapotranspiration has a significant impact, it suggests that either the related
289 formulation in the GR4J model or the observations may require further investigation.

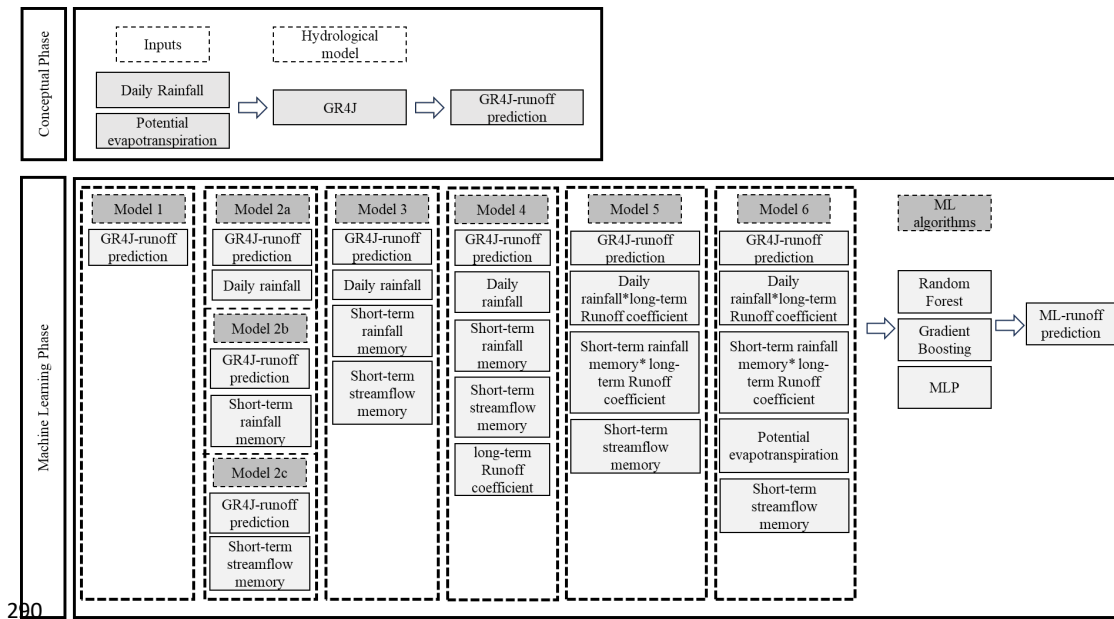


Figure 3 Schematic of the applied methodology.

The performance of the GR4J and ML models was assessed using the Nash-Sutcliffe Efficiency (NSE) and NSE of log-transformed flows. To assess the model performance for low-flows, the NSE of log-transformed flow was investigated, because logarithmic transformation increases the sensitivity of model performance assessment to low flow values (Romanowicz, 2007). To provide insight into the performance across the range of catchments investigated, exceedance curves for performance measures were generated. Where an ensemble of ML models is established, an ensemble of predictions is generated, one for each model, the NSE computed separately for each ensemble member and then averaged to produces a mean NSE value across the prediction ensemble.

The classification system for NSE of daily flow simulations devised by (Moriassi et al., 2015) was used to categorise model performance Table 1.

Table 1. Model performance evaluation criteria for daily flow, based on the NSE value.

Very good	Good	Satisfactory	Not Satisfactory
$NSE > 0.80$	$0.70 < NSE \leq 0.80$	$0.50 < NSE \leq 0.70$	$NSE \leq 0.50$



Sensitivity analyses were conducted to evaluate the impact of varying two parameters: the number of days considered for short-term pre-streamflow in model 2c and the duration of years used to calculate the long-term runoff coefficient in model 5. Specifically, the analysis examined short-term periods ranging from 2 to 7 days while keeping the long-term period fixed at 5 years, and separately, long-term periods spanning 1 to 5 years with a fixed short-term period of 2 days, to assess how these variables affect model performance and prediction accuracy.

3 Results and discussion

The focus of this study is to understand the additional information required to improve streamflow simulations in a period with different rainfall-runoff characteristics for fitting models. Therefore, we firstly assess the differences in mean daily rainfall and runoff between the model training and prediction periods (Figure 4). The decrease in the streamflow across all sub-catchments in this region is considerably larger than the reduction in the precipitation. This observation highlights the significance of this region as a proper case study, prompting further investigation to understand the underlying reasons for this discrepancy.

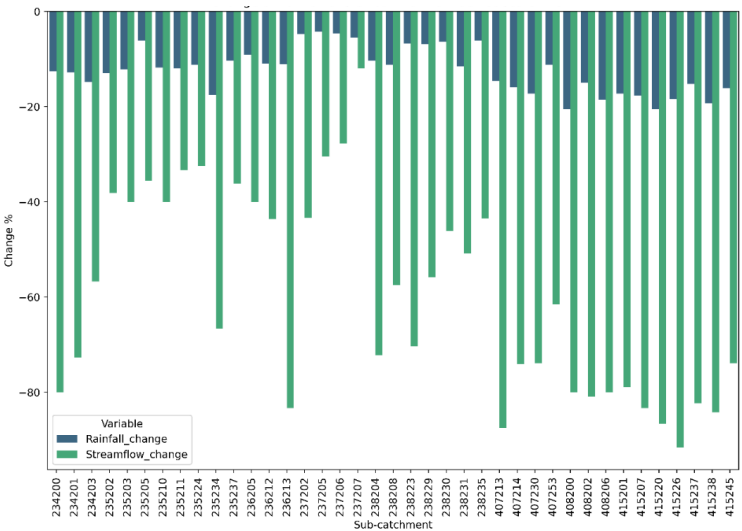
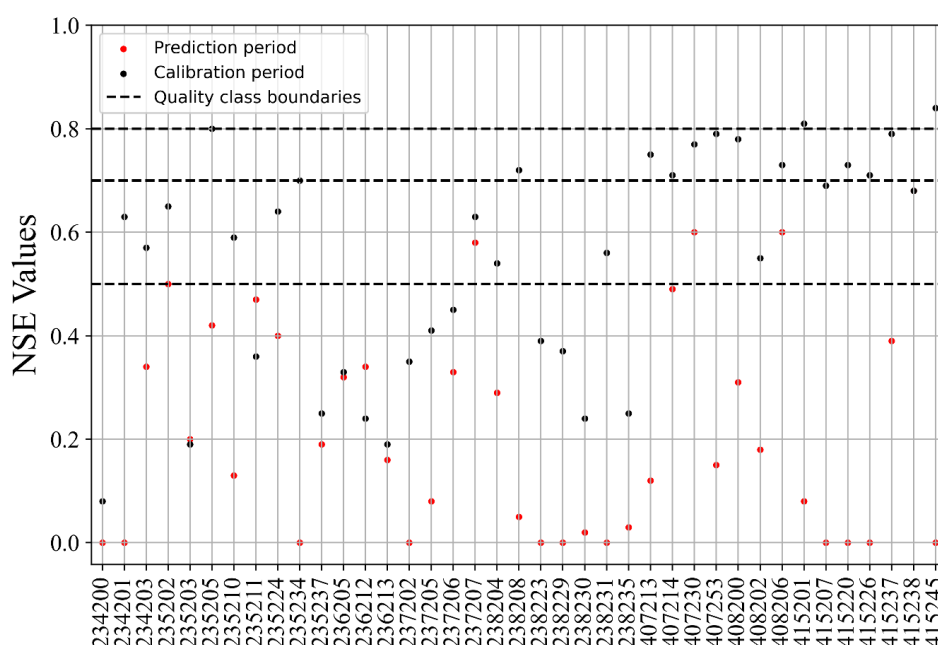


Figure 4. Comparison of the mean daily rainfall and streamflow change from 1988-01-01 to 1996-12-31 (pre-drought) and from 1997-01-01 to 2018-12-31 (drought and post-drought).



320 The NSE values of the GR4J hydrological model predictions during the drought and post-drought
 321 prediction periods are shown in Figure 5. The NSE for the prediction period are considerably lower
 322 than the calibration period for all catchments. For the prediction period, the performance of the GR4J
 323 hydrological model simulations can be classified as “satisfactory” for only 5 sub-catchments, with the
 324 remainder “not satisfactory”.



325

326 *Figure 5 NSE values of the GR4J hydrological model, for the calibration period and prediction of drought and post-drought*
 327 *periods when calibrated to the pre-drought period. The horizontal dashed lines represent the boundary between the*
 328 *performance classes as defined in Table 1. Negative values are shown as zero in this figure.*

329 The performance of the three ML algorithms across the study catchments is presented as the exceedance
 330 probability curves in Figure 6. For each value of the NSE in the X-axis, this curve shows the percentage
 331 of the sub-catchments that have an NSE value higher than this specific value. A larger area under the
 332 curve thus indicates a better model performance and for enhanced clarity, negative values are omitted.
 333 None of the models 1, 2a, and 2b show any improvement over the GR4J predictions, whereas for model
 334 2c all ML algorithms lead to a clear improvement. Model 2c is analogous to a deterministic error
 335 correction model that uses recent streamflow observations to update GR4J predictions. MLP, Random



336 Forest, and Gradient Boosting exhibit consistent improvement for both Model 5 and Model 6 in around
337 90% of the sub-catchments. MLP exhibits the strong overall performance for all models, which can be
338 attributed to the non-linear nature of the problem, where MLP excels in addressing nonlinearity. To
339 show and compare the performance of models with the best performing ML algorithms in each gauge,
340 box plots of 10 ensemble members are provided in the Appendix, Figure A. 2.

341 For a better understanding of the behaviour of the eight proposed models, exceedance probability curves
342 depicting mean NSE values are provided in Figure 7. Model 2c demonstrates improvement with respect
343 to GR4J, which emphasises the importance of taking into account short-term streamflow memory.
344 Model 3 shows improvement with respect to model 2c, which indicates the importance of short-term
345 rainfall and streamflow memory and daily rainfall combination. Model 5 and Model 6 clearly
346 outperform Model 3. While model 4 does not show improvement to model 3. This suggests that
347 affecting long-term runoff coefficient to rainfall and short-term rainfall memory can play a crucial role
348 in improving daily streamflow predictions, and therefore the GR4J model would appear to be lacking
349 the ability to represent long-term rainfall-runoff dynamics. Using the MLP algorithm, the performance
350 of Model 5 and Model 6 is relatively similar, indicating that using potential evapotranspiration as a
351 predictor adds little value to the predictions.

352

353

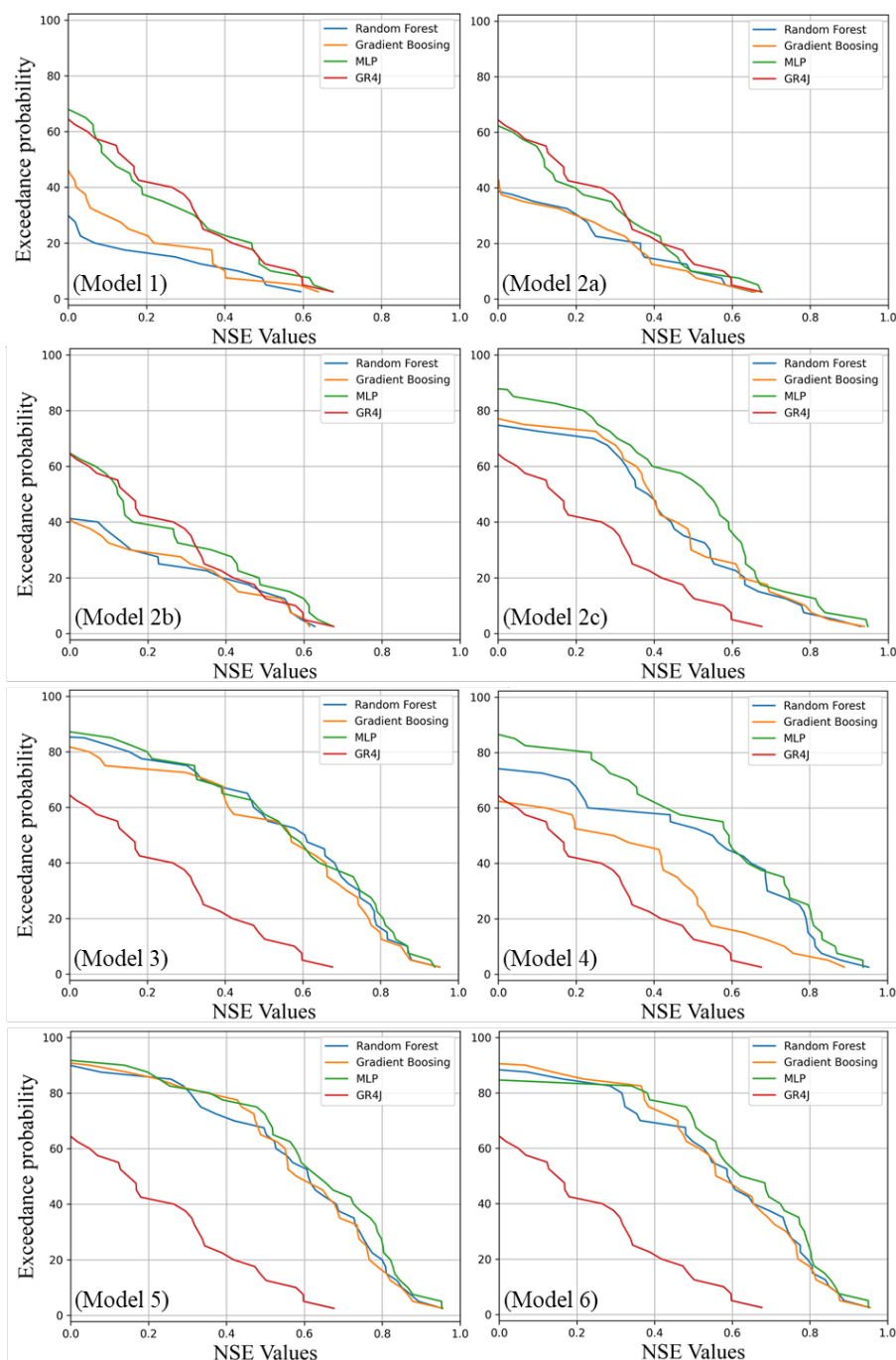
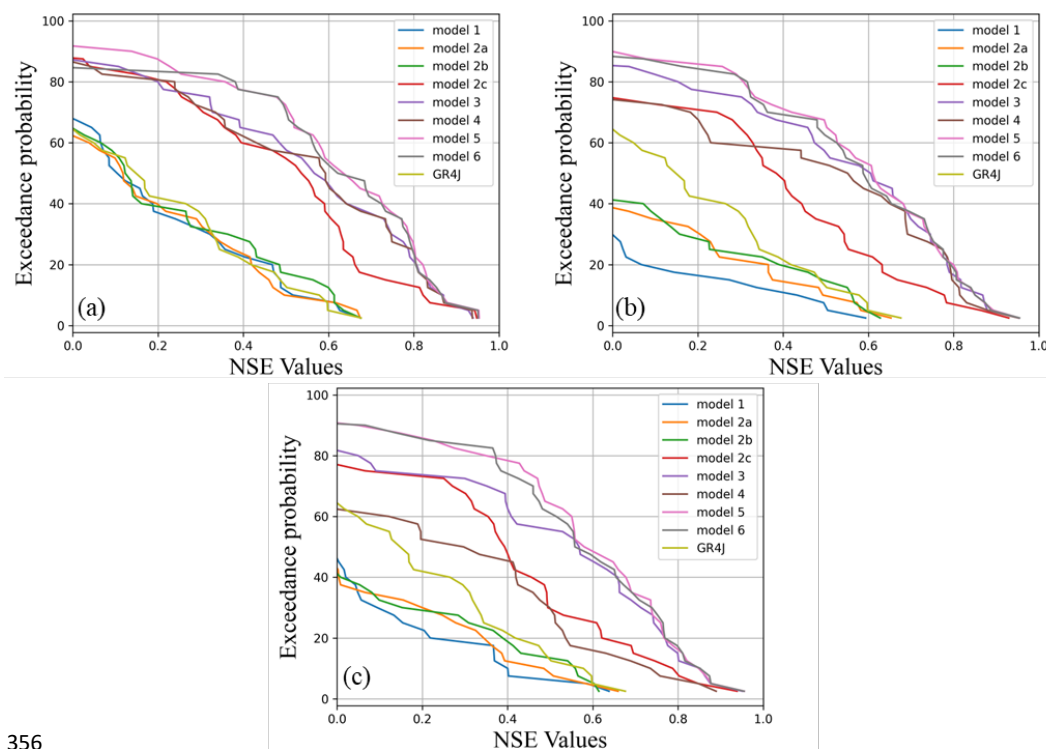


Figure 6 Exceedance probability curves of the mean NSE values for different ML algorithms for All models.



356

357 *Figure 7 Exceedance probability curves of mean NSE values of different models by application of different algorithms a)*

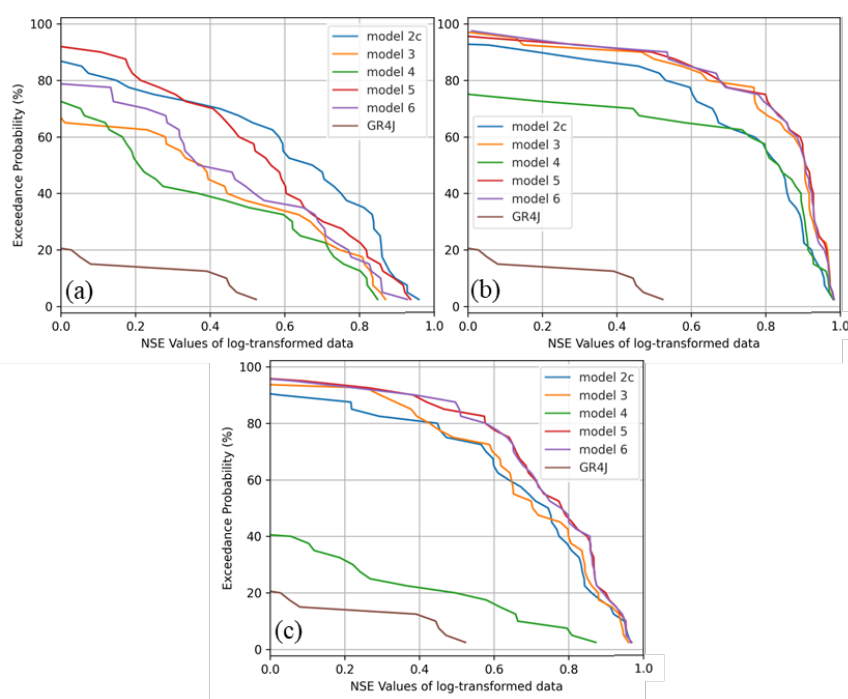
358 *MLP, b) Random forest, and c) Gradient boosting.*

359 In some sub-catchments, despite the considerable improvement of the NSE in comparison to GR4J,
360 there are still unsatisfactory results, NSE values less than 0.5 for approximately 30% of sub-catchments,
361 indicating the potential for further enhancement. This suggests that other parameters, such as NDVI,
362 LAI, groundwater exchange, etc., should be considered as predictor in future studies.

363 The low-flow performance of the ML models assessed in Figure 8 and Figure 9. The exceedance
364 probability curves for the NSE of log-transformed streamflow for the ML models and GR4J results are
365 presented in Figure 8. All ML algorithms produce more accurate low flow predictions than GR4J. In
366 contrast to the results for NSE, Random Forest demonstrates the greatest ability to improve low-flow
367 predictions. Model 2c showed generally better performance compared to the other models when using
368 the MLP algorithm. Models 3, 5, and 6 performed similarly with the Random Forest algorithms and
369 better than models 2c and 4. When Gradient Boosting was applied, both Model 5 and Model 6 yielded



370 similar results, surpassing other models, while model 4 showed very poor performance. These
371 enhancements underscore the effectiveness of machine learning and highlight how predictors and
372 algorithms influence low-flow streamflow predictions. Consequently, it appears that the GR4J model
373 lacks the capability to adequately represent long-term rainfall-runoff and short-term rainfall and runoff
374 dynamics, particularly in the context of low flows.



375

376 *Figure 8 Exceedance probability curves of mean NSE values of log-transformed streamflow, for different models by*
377 *application of different algorithms a) MLP, b) Random Forest, and c) Gradient boosting.*

378 Figure 9 represents the heatmap of log-transformed observations vs log-transformed predictions for
379 model 3, 5, and 6, as the best performed models. The colour of each cell represents the number of
380 observation-prediction pairs in that cell. Overall, the GR4J model tends to overestimate predictions for
381 lower streamflow. The application of ML algorithms resulted in more symmetrical shape compared to
382 GR4J, with ML predictions more closely following the identity line, indicating improved prediction
383 accuracy. However, in the case of MLP, the darker coloration of cells for log-transformed observations
384 and ML predictions below -4 suggests two issues: the former indicates overestimation of some zero-



385 flow observations, while the latter indicates no-flow predictions for days with actual streamflow. This
386 undesired behaviour was mitigated using other algorithms, with Random Forest demonstrating the best
387 performance among the candidates. Furthermore, the darker and narrower area around the equity line
388 in the Random Forest figures, particularly at lower log-transformed values, highlights significant
389 prediction improvement. However, the difference between models remains indistinct, indicating that
390 while low-flow prediction has improved, it is not evident which predictor has the greatest overall
391 impact. These results underscore the significant influence of applying ML specifically to low-flow
392 conditions, which is the primary focus of this study, i.e., the Millennium drought.

393

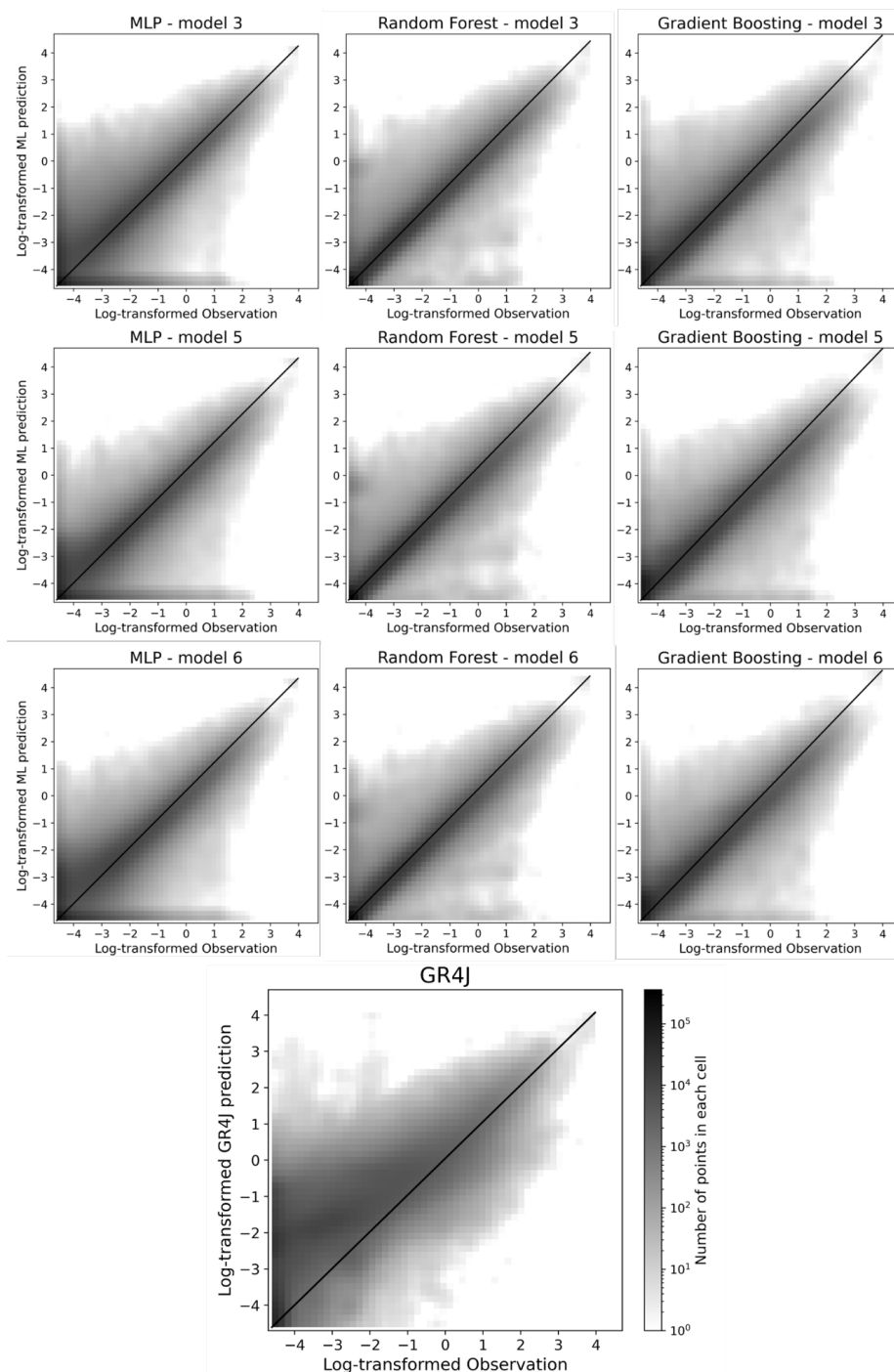
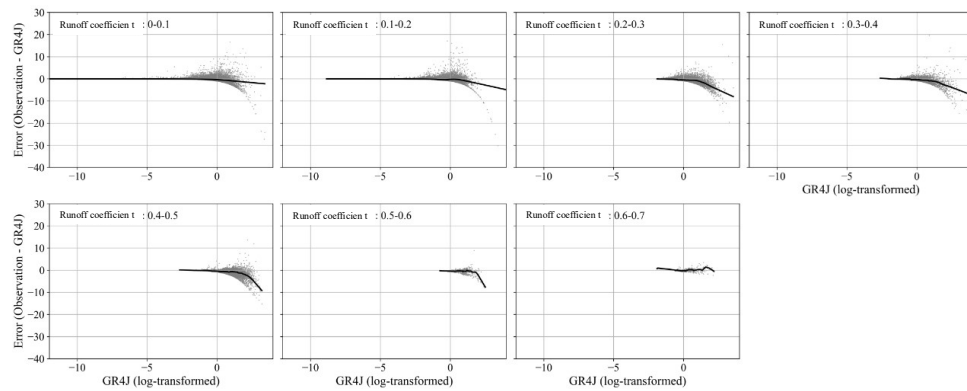


Figure 9 Heatmap of the log-transformation result



396 To better understand the role of long-term runoff coefficient in improving streamflow predictions it is
397 examined how errors in GR4J simulations vary with the long-term runoff coefficient (Figure 10), and
398 how the MLP Model 5, as the best performed model, uses the long-term runoff coefficient to improve
399 streamflow predictions (Figure 11). Overall, the GR4J streamflow simulations cover a wide range of
400 values for all ranges of the long-term runoff coefficient, although few low streamflow values simulated
401 when the long-term runoff coefficient is high. Errors tend to be small for low GR4J streamflow
402 simulations, however for higher streamflow simulations the errors vary with the value of the long-term
403 runoff coefficient. For values of the long-term runoff coefficient (0 to 0.4), GR4J underestimates lower
404 flows and overestimates higher flows. In the 0.4–0.5 range, GR4J predominantly shows
405 overestimations. However, there are no clear patterns for long-term runoff coefficients in the 0.5–0.7
406 range, where GR4J simulations exhibit small errors. These results indicate that the magnitude of errors
407 in simulated streamflow vary with the long-term runoff coefficient, particularly for simulations of
408 higher streamflow.

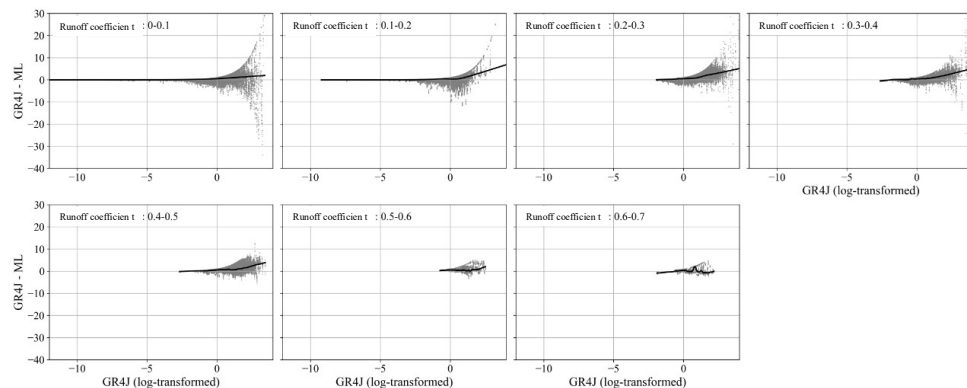
409 The ML method corrects the streamflow simulations to reduce these error patterns, by increasing
410 simulations of large streamflow where the long-term runoff coefficient range (0.0 to 0.4). The ML
411 method makes little correction to streamflow predictions when the long-term runoff coefficient is larger
412 than 0.5. The corrections related to the long-term runoff coefficient being applied by the ML method,
413 to the GR4J simulations, are in addition to corrections related to short-term streamflow memory.
414 Therefore, the results are suggesting that GR4J simulation errors are dependent on the prevailing long-
415 term hydrological conditions, and specifically related to the ability of GR4J to simulate high streamflow
416 during dry conditions. Therefore, the analysis provides insights into structural weaknesses in the GR4J
417 model for the catchments investigated in this study.



418

419 *Figure 10 GR4J error categorized based on long-term runoff coefficient ranges. Solid line represents a LOWESS (locally*
420 *weighted scatterplot smoothing) line of best fit.*

421



422

423 *Figure 11 GR4J and ML(MLP model5) difference categorized based on long-term runoff coefficient ranges. Solid line*
424 *represents a LOWESS (locally weighted scatterplot smoothing) line of best fit.*

425

426 Sensitivity analysis of the short-term streamflow memory predictor to the duration over which the
427 predictor is computed indicates that shorter durations lead to slight improvements in NSE values (Figure
428 A. 3). This improvement is likely due to the increased relevance of recent streamflow conditions in
429 error correction and model prediction. In contrast, for the long-term runoff coefficient, the results show
430 no significant differences, and no clear pattern emerges between different durations (Figure A. 4). This
431 lack of consistency suggests that the influence of the long-term runoff coefficient is highly dependent
432 on the specific characteristics of the sub-catchment, with variations observed across different sub-
433 catchments.



434

435 **4 Conclusion**

436 This study has investigated streamflow prediction before, during and after the Millennium drought
437 (1997 to 2009) in catchments of Western Victoria, Australia. The GR4J hydrological model was found
438 to produce poor streamflow predictions for the drought and post-drought periods when calibrated to
439 pre-drought conditions. Multiple machine learning methods were used to investigate possible
440 improvements to streamflow predictions, using GR4J model simulations and physical data as predictors.
441 Eight combinations of predictors were considered. All ML algorithms investigated improved the
442 streamflow prediction for the drought and post-drought period in comparison to GR4J when trained
443 using data for the pre-drought period. MLP, Gradient Boosting, and Random Forest produced
444 simulations with greater accuracy overall and for low flow conditions than Linear Regression, Ridge
445 Regression, SVR, and Decision Tree. The better performing ML methods have greater ability to
446 characterise non-linear relationships between predictors and streamflow, than the poorer performing
447 methods, suggesting that the calibrated GR4J model inadequately resolving some non-linear rainfall-
448 runoff processes in the study sub-catchments.

449 Model 5 that combines predictors representing short-term memories and product of long-term runoff
450 coefficient and rainfall without considering potential evapotranspiration as predictor showed the
451 greatest improvements in prediction accuracy. This model improved streamflow predictions for around
452 90% of the sub-catchments using MLP, Random Forest, and Gradient Boosting algorithms. The
453 improvements in streamflow predictions arising from the use of long-term runoff coefficient as
454 predictors for the machine learning models suggests that the calibrated GR4J models inadequately
455 represent the slow or long-term dynamics of rainfall-runoff processes. These slow dynamics would
456 therefore appear to be critical for modelling low streamflow, particularly those that occur during drought
457 periods.

458 In this study, models were training using only data for the pre-drought period that was wetter than the
459 drought and post-drought periods on which their performance was assessed. The calibrated GR4J



models showed considerably poorer performance during the drought and post-drought periods. However, the predictions from the ML models, when trained using data for the same period, were able to produce predictions for the drought and post-drought periods that are considerably more accurate than the GR4J model. The better performing ML models used a combination of the GR4J simulations and long-term/short-term variables as predictors. The improved performance of the ML model predictions for the post-drought period relative to those of GR4J, indicate that the long-term and short-term streamflow memory effects exist in the pre-drought period. Therefore, it should be possible to introduce modifications to the GR4J model, used here, to better represent the dynamics related to long-term and short-term variables. It is found that consideration of long-term runoff coefficient and application of ML are most suitable for catchments with low runoff coefficient. As such, this study underscores the important role that ML methods can play in identifying directions for improving models used for streamflow prediction, particularly under variable climatic conditions in drought-prone regions.

Authorship contribution statement

Arash Aghakhani: Conceptualization, Data curation, Formal analysis, Methodology, Investigation, Software, Validation, Writing - original draft, Writing - review & editing

David Robertson: Conceptualization, Data curation, Formal analysis, Methodology, Funding acquisition, Resources, Supervision, Validation, Writing - review & editing

Valentijn Pauwels: Conceptualization, Formal analysis, Methodology, Funding acquisition, Supervision, Validation, Writing - review & editing

Declaration of Competing Interest

"The authors declare that they have no conflict of interest."

Data availability

Code will be available on GitHub. HRS stations data are available at (Hydrologic Reference Stations, 2024)

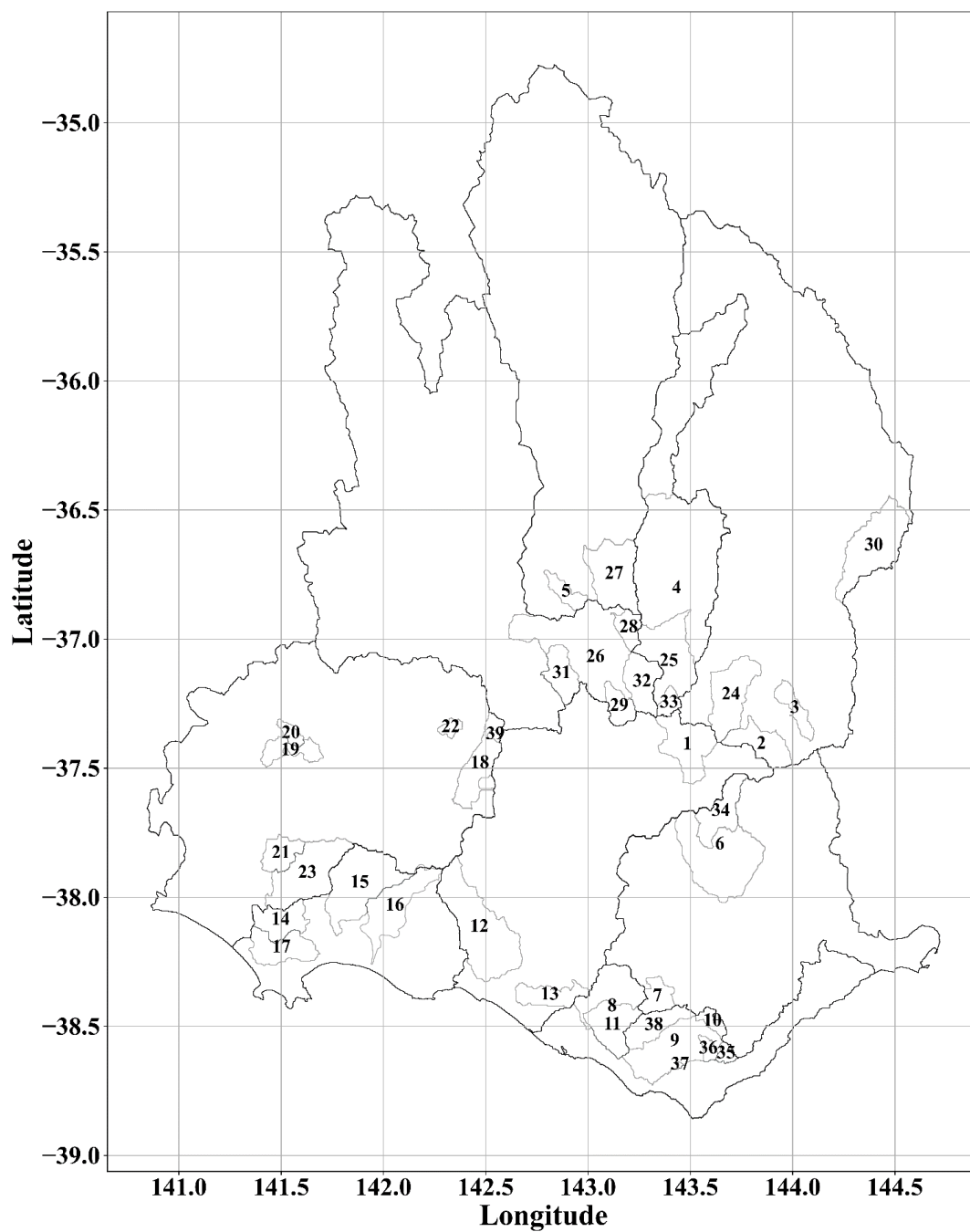


485 **Acknowledgement**

486 This work was conducted on the traditional lands of the Boonwurrung peoples of the Kulin Nation. We
487 acknowledge their continuing custodianship of these lands and the rivers that flow through them, and
488 pay our respects to their elders, past and present. We also acknowledge the traditional custodians of the
489 catchments and rivers used in this study. This research has been supported by Monash University and
490 CSIRO.



491 5 Appendix



492

493 *Figure A. 1 Geographical representation of study area*



494

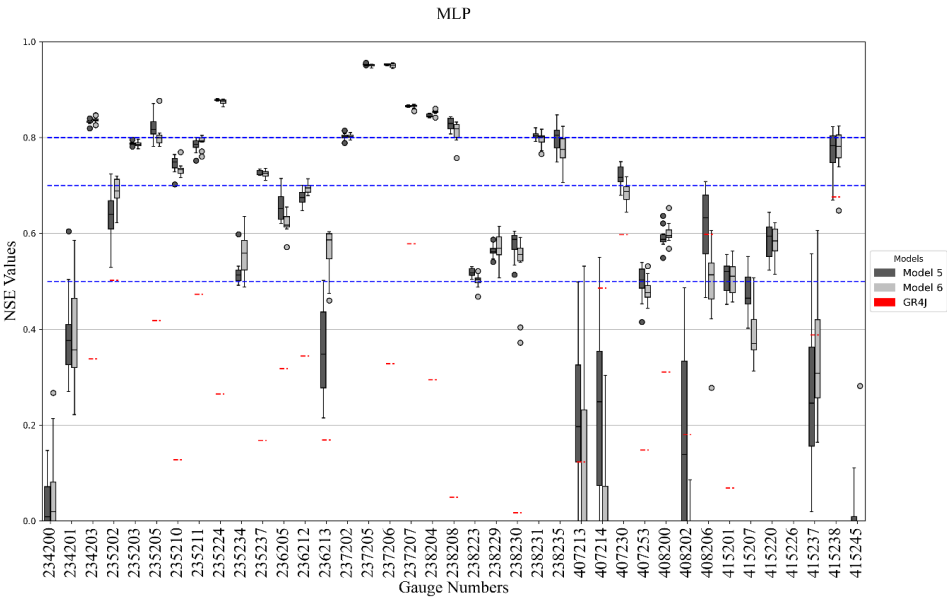
495 *Table A. 1 Sub-catchments general information*

Sub-catchment	Station No.	Gauge Name	Area of sub-catchment (km ²)	Catchment Name
1	236213	Mena Park	448.3	Hopkins River
2	407214	Clunes	299.9	Loddon River
3	407230	Strathlea	156	Loddon River
4	408200	Coonooer	2677.3	Avoca River
5	415226	Carrs Plains	124.9	Avon River-Tyrell lake
6	234201	Cressy (Yarima)	1166.5	Barwon River-Lake Corangamite
7	234203	Pirron Yallock (above H'Wy	161.3	Barwon River-Lake Corangamite
8	235203	Curdie	721.3	Otway Coast
9	235224	Burrupa	1042	Otway Coast
10	235234	Gellibrand	76.6	Otway Coast
11	235237	Curdie (Digneys Br)	340.3	Otway Coast
12	236205	Woodford	893.1	Hopkins River
13	236212	Cudgee	225.4	Hopkins River
14	237202	Heywood	268.1	Portland Coast
15	237205	Homerton Br	713.7	Portland Coast
16	237206	Codrington	474	Portland Coast
17	237207	Heathmere	312.4	Portland Coast
18	238204	Dunkeld	384.9	Glenelg River
19	238223	Wando Vale	180.2	Glenelg River
20	238229	Chetwynd	69	Glenelg River
21	238230	Teakettle	197	Glenelg River
22	238231	Big Cord	54	Glenelg River
23	238235	Lower Crawford	600.8	Glenelg River
24	407213	Carisbrook	471.5	Loddon River
25	408206	Archdale Junction	760.6	Avoca River
26	415201	Glenorchy Weir Tail Gauge	1976.1	Wimmera River
27	415220	Wimmera HWY	543	Avon River-Tyrell lake
28	415238	Navarre	139.7	Wimmera River
29	415245	Crowlands	159.2	Wimmera River
30	407253	Minto	652.1	Loddon River
31	415237	Stawell	244.2	Wimmera River
32	415207	Eversley	304.5	Wimmera River



Sub-catchment	Station No.	Gauge Name	Area of sub-catchment (km2)	Catchment Name
33	408202	Amphitheatre	82.6	Avoca River
34	234200	Pitfield	316.9	Barwon River-Lake Corangamite
35	235202	Upper Gellibrand	52.7	Otway Coast
36	235210	Gellibrand	53.9	Otway Coast
37	235205	Wyelangta	4.5	Otway Coast
38	235211	Kennedys Ck	263.7	Otway Coast
39	238208	Jimmy Creek	23.3	Glenelg River

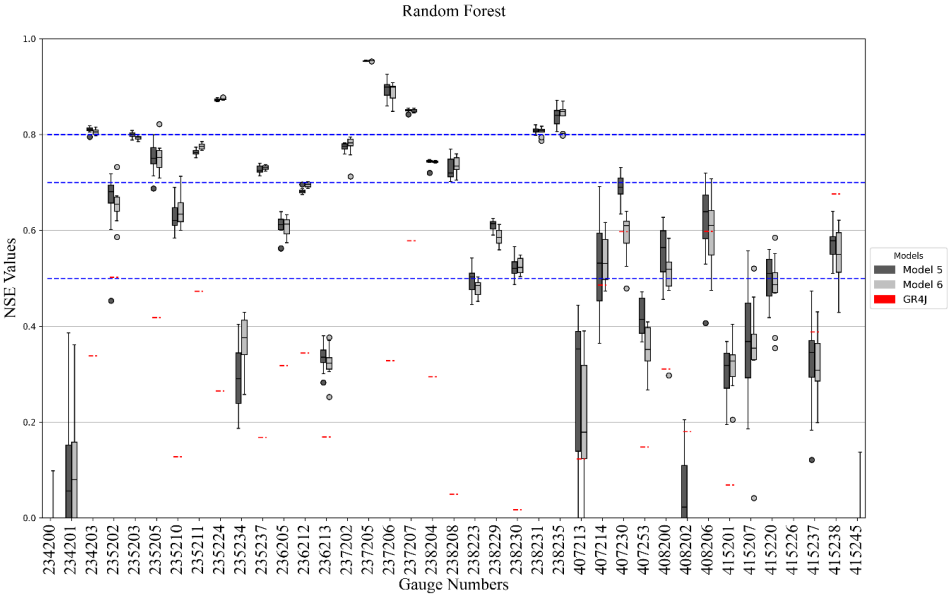
496



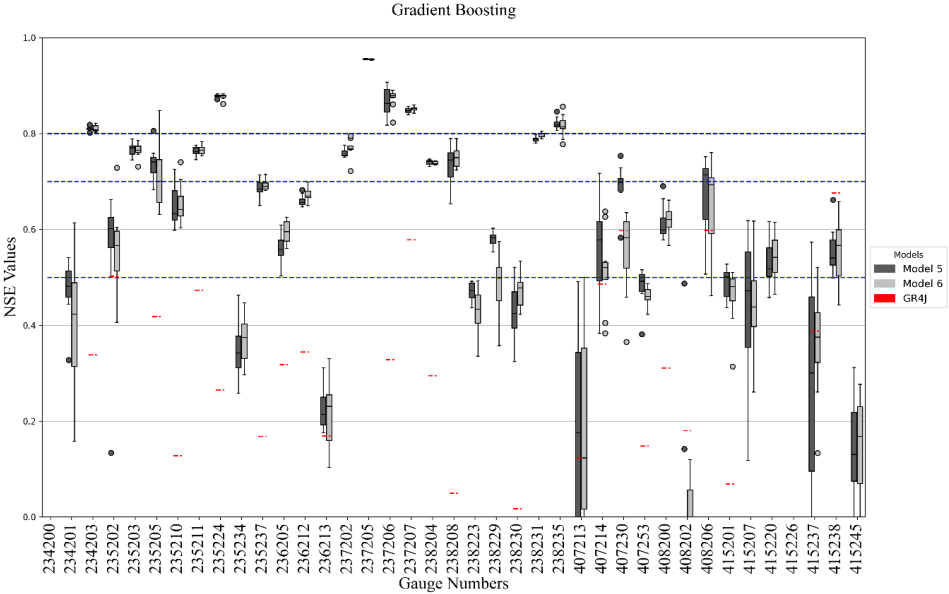
497



498



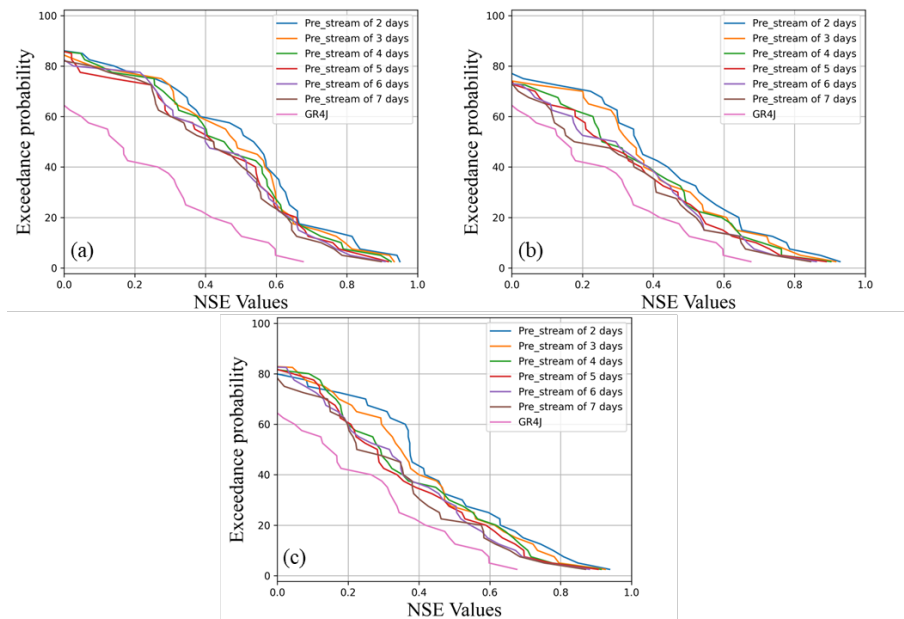
499



500 *Figure A. 2 box plots of NSE values of 10 repeats*

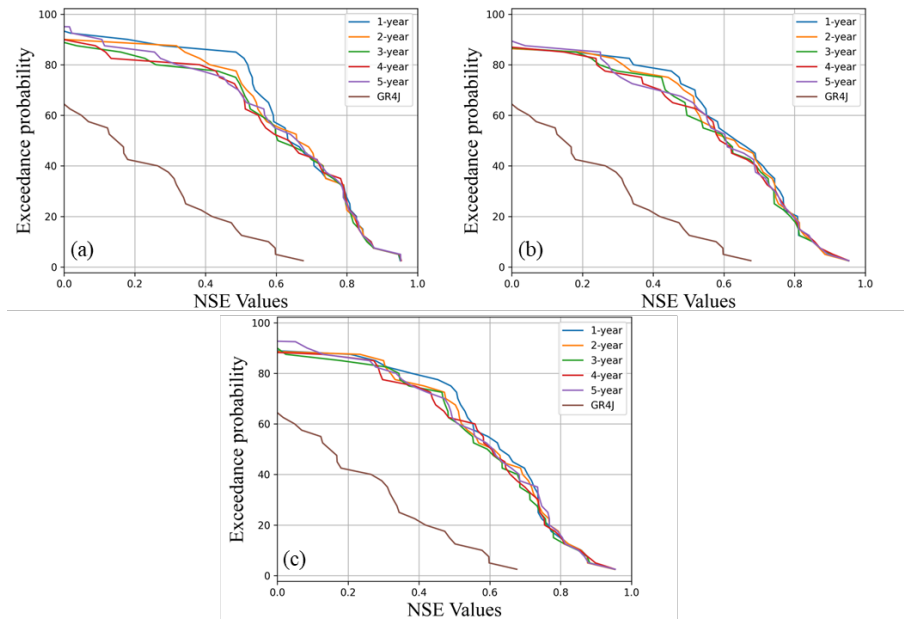
501

502



503

504 *Figure A. 3 Sensitivity analysis of short-term pre-stream (days), a) MLP, b) Random Forest, and c) Gradient boosting.*



505

506 *Figure A. 4 Sensitivity analysis of Long-term runoff coefficient (years), a) MLP, b) Random Forest, and c) Gradient boosting*



507 6 References

- 508 Akusok, A., Bjork, K. M., Miche, Y., and Lendasse, A.: High-Performance Extreme Learning Machines:
509 A Complete Toolbox for Big Data Applications, IEEE Access, 3,
510 <https://doi.org/10.1109/ACCESS.2015.2450498>, 2015.
- 511 Arsenault, R., Breton-Dufour, M., Poulin, A., Dallaire, G., and Romero-Lopez, R.: Streamflow
512 prediction in ungauged basins: analysis of regionalization methods in a hydrologically heterogeneous
513 region of Mexico, Hydrological Sciences Journal, 64,
514 <https://doi.org/10.1080/02626667.2019.1639716>, 2019.
- 515 Aryal, S. K., Zhang, Y., and Chiew, F.: Enhanced low flow prediction for water and environmental
516 management, J Hydrol (Amst), 584, <https://doi.org/10.1016/j.jhydrol.2020.124658>, 2020.
- 517 Ayzel, G., Kurochkina, L., Abramov, D., and Zhuravlev, S.: Development of a regional gridded runoff
518 dataset using long short-term memory (LSTM) networks, Hydrology, 8,
519 <https://doi.org/10.3390/hydrology8010006>, 2021.
- 520 Bentéjac, C., Csörgő, A., and Martínez-Muñoz, G.: A comparative analysis of gradient boosting
521 algorithms, Artif Intell Rev, 54, <https://doi.org/10.1007/s10462-020-09896-5>, 2021.
- 522 Biau, G., Cadre, B., and Rouvière, L.: Accelerated gradient boosting, Mach Learn, 108,
523 <https://doi.org/10.1007/s10994-019-05787-1>, 2019.
- 524 Blöschl, G., Bierkens, M. F. P., Chambel, A., Cudennec, C., Destouni, G., Fiori, A., Kirchner, J. W.,
525 McDonnell, J. J., Savenije, H. H. G., Sivapalan, M., Stumpp, C., Toth, E., Volpi, E., Carr, G., Lupton, C.,
526 Salinas, J., Széles, B., Viglione, A., Aksoy, H., Allen, S. T., Amin, A., Andréassian, V., Arheimer, B., Aryal,
527 S. K., Baker, V., Bardsley, E., Barendrecht, M. H., Bartosova, A., Batelaan, O., Berghuijs, W. R., Beven,
528 K., Blume, T., Bogaard, T., Borges de Amorim, P., Böttcher, M. E., Boulet, G., Breinl, K., Brilly, M.,
529 Brocca, L., Buytaert, W., Castellarin, A., Castelletti, A., Chen, X., Chen, Y., Chen, Y., Chiffard, P., Claps,
530 P., Clark, M. P., Collins, A. L., Croke, B., Dathe, A., David, P. C., de Barros, F. P. J., de Rooij, G., Di
531 Baldassarre, G., Driscoll, J. M., Duethmann, D., Dwivedi, R., Eris, E., Farmer, W. H., Feicabrino, J.,
532 Ferguson, G., Ferrari, E., Ferraris, S., Fersch, B., Finger, D., Foglia, L., Fowler, K., Gartsman, B., Gascoin,
533 S., Gaume, E., Gelfan, A., Geris, J., Gharari, S., Gleeson, T., Glendell, M., Gonzalez Bevacqua, A.,
534 González-Dugo, M. P., Grimaldi, S., Gupta, A. B., Guse, B., Han, D., Hannah, D., Harpold, A., Haun, S.,
535 Heal, K., Helfricht, K., Herrnegger, M., Hipsey, M., Hlaváčiková, H., Hohmann, C., Holko, L., Hopkinson,
536 C., Hrachowitz, M., Illangasekare, T. H., Inam, A., Innocente, C., Istanbuluoglu, E., Jarihani, B., et al.:
537 Twenty-three unsolved problems in hydrology (UPH)—a community perspective, Hydrological
538 Sciences Journal, 64, <https://doi.org/10.1080/02626667.2019.1620507>, 2019.
- 539 Boucher, M. A., Quilty, J., and Adamowski, J.: Data Assimilation for Streamflow Forecasting Using
540 Extreme Learning Machines and Multilayer Perceptrons, Water Resour Res, 56,
541 <https://doi.org/10.1029/2019WR026226>, 2020.
- 542 Bureau of Meteorology, Previous droughts: [http://www.bom.gov.au/climate/drought/knowledge-](http://www.bom.gov.au/climate/drought/knowledge-centre/previous-droughts.shtml)
543 [centre/previous-droughts.shtml](http://www.bom.gov.au/climate/drought/knowledge-centre/previous-droughts.shtml), last access: 28 May 2024.
- 544 Hydrologic Reference Stations: <http://www.bom.gov.au/water/hrs/>, last access: 1 February 2024.



- 545 Cheng, M., Fang, F., Kinouchi, T., Navon, I. M., and Pain, C. C.: Long lead-time daily and monthly
546 streamflow forecasting using machine learning methods, *J Hydrol (Amst)*, 590,
547 <https://doi.org/10.1016/j.jhydrol.2020.125376>, 2020.
- 548 Chiew, F. H. S., Potter, N. J., Vaze, J., Petheram, C., Zhang, L., Teng, J., and Post, D. A.: Observed
549 hydrologic non-stationarity in far south-eastern Australia: Implications for modelling and prediction,
550 *Stochastic Environmental Research and Risk Assessment*, 28, [https://doi.org/10.1007/s00477-013-](https://doi.org/10.1007/s00477-013-0755-5)
551 0755-5, 2014.
- 552 Southwest Victoria alliance-Advocacy Priorities 2021/22:
553 https://treasury.gov.au/sites/default/files/2022-03/258735_southwest_victoria_alliance.pdf, last
554 access: 28 March 2024.
- 555 Deo, R. C. and Şahin, M.: An extreme learning machine model for the simulation of monthly mean
556 streamflow water level in eastern Queensland, *Environ Monit Assess*, 188,
557 <https://doi.org/10.1007/s10661-016-5094-9>, 2016.
- 558 Van Dijk, A. I. J. M., Beck, H. E., Crosbie, R. S., De Jeu, R. A. M., Liu, Y. Y., Podger, G. M., Timbal, B., and
559 Viney, N. R.: The Millennium Drought in southeast Australia (2001-2009): Natural and human causes
560 and implications for water resources, ecosystems, economy, and society, *Water Resour Res*, 49,
561 <https://doi.org/10.1002/wrcr.20123>, 2013.
- 562 Duan, Q., Sorooshian, S., and Gupta, V. K.: Optimal use of the SCE-UA global optimization method for
563 calibrating watershed models, *J Hydrol (Amst)*, 158, [https://doi.org/10.1016/0022-1694\(94\)90057-4](https://doi.org/10.1016/0022-1694(94)90057-4),
564 1994.
- 565 Fowler, K., Peel, M., Saft, M., Peterson, T. J., Western, A., Band, L., Petheram C., Dharmadi, S., Tan, K.
566 S., Zhang, L., and Lane, P.: Explaining changes in rainfall–runoff relationships during and after
567 Australia’s Millennium Drought: a community perspective, *Hydrology and Earth System Sciences*, 26,
568 6073–6120, 2022.
- 569 Fowler, K. J. A., Coxon, G., Freer, J. E., Knoben, W. J. M., Peel, M. C., Wagener, T., Western, A. W.,
570 Woods, R. A., and Zhang, L.: Towards more realistic runoff projections by removing limits on
571 simulated soil moisture deficit, *J Hydrol (Amst)*, 600, <https://doi.org/10.1016/j.jhydrol.2021.126505>,
572 2021.
- 573 Frost, A. J. , and D. P. W.: Evaluation of the Australian landscape water balance model: AWRA-L v6.,
574 Melbourne, VIC, Australia, 2018.
- 575 Hao, R. and Bai, Z.: Comparative Study for Daily Streamflow Simulation with Different Machine
576 Learning Methods, *Water (Switzerland)*, 15, <https://doi.org/10.3390/w15061179>, 2023.
- 577 He, X., Luo, J., Li, P., Zuo, G., and Xie, J.: A Hybrid Model Based on Variational Mode Decomposition
578 and Gradient Boosting Regression Tree for Monthly Runoff Forecasting, *Water Resources*
579 *Management*, 34, <https://doi.org/10.1007/s11269-020-02483-x>, 2020.
- 580 Heberger, M.: Australia’s Millennium Drought: Impacts and Responses, in: *The World’s Water*,
581 https://doi.org/10.5822/978-1-59726-228-6_5, 2012.
- 582 Jones, D. A., Wang, W., and Fawcett, R.: High-quality spatial climate data-sets for Australia, *Australian*
583 *Meteorological and Oceanographic Journal*, 58, <https://doi.org/10.22499/2.5804.003>, 2009.



- 584 Konapala, G., Kao, S. C., Painter, S. L., and Lu, D.: Machine learning assisted hybrid models can
585 improve streamflow simulation in diverse catchments across the conterminous US, *Environmental*
586 *Research Letters*, 15, <https://doi.org/10.1088/1748-9326/aba927>, 2020.
- 587 Kumar, V., Kedam, N., Sharma, K. V., Mehta, D. J., and Caloiero, T.: Advanced Machine Learning
588 Techniques to Improve Hydrological Prediction: A Comparative Analysis of Streamflow Prediction
589 Models, *Water (Switzerland)*, 15, <https://doi.org/10.3390/w15142572>, 2023.
- 590 Lees, T., Buechel, M., Anderson, B., Slater, L., Reece, S., Coxon, G., and Dadson, S. J.: Benchmarking
591 data-driven rainfall-runoff models in Great Britain: A comparison of long short-term memory (LSTM)-
592 based models with four lumped conceptual models, *Hydrol Earth Syst Sci*, 25,
593 <https://doi.org/10.5194/hess-25-5517-2021>, 2021.
- 594 Li, M., Zhang, Y., Wallace, J., and Campbell, E.: Estimating annual runoff in response to forest change:
595 A statistical method based on random forest, *J Hydrol (Amst)*, 589,
596 <https://doi.org/10.1016/j.jhydrol.2020.125168>, 2020.
- 597 Lima, A. R., Cannon, A. J., and Hsieh, W. W.: Forecasting daily streamflow using online sequential
598 extreme learning machines, *J Hydrol (Amst)*, 537, <https://doi.org/10.1016/j.jhydrol.2016.03.017>,
599 2016.
- 600 Mohammadi, B., Ahmadi, F., Mehdizadeh, S., Guan, Y., Pham, Q. B., Linh, N. T. T., and Tri, D. Q.:
601 Developing Novel Robust Models to Improve the Accuracy of Daily Streamflow Modeling, *Water*
602 *Resources Management*, 34, <https://doi.org/10.1007/s11269-020-02619-z>, 2020.
- 603 Moosavi, V., Gheisoori Fard, Z., and Vafakhah, M.: Which one is more important in daily runoff
604 forecasting using data driven models: Input data, model type, preprocessing or data length?, *J Hydrol*
605 *(Amst)*, 606, <https://doi.org/10.1016/j.jhydrol.2022.127429>, 2022.
- 606 Moriasi, D. N., Gitau, M. W., Pai, N., and Daggupati, P.: Hydrologic and water quality models:
607 Performance measures and evaluation criteria, *Trans ASABE*, 58,
608 <https://doi.org/10.13031/trans.58.10715>, 2015.
- 609 Ng, K. W., Huang, Y. F., Koo, C. H., Chong, K. L., El-Shafie, A., and Najah Ahmed, A.: A review of hybrid
610 deep learning applications for streamflow forecasting, *J Hydrol (Amst)*, 625, 130141,
611 <https://doi.org/10.1016/j.jhydrol.2023.130141>, 2023.
- 612 Onyari, E. and Ilunga, F.: Application of MLP neural network and M5P model tree in predicting
613 streamflow: A case study of Luvuvhu catchment, South Africa, *ijimt.org*, 2013.
- 614 Perraud, J. M., Bennett, J. C., Bridgart, R., and Robertson, D.: SWIFT2: Advanced software for
615 continuous ensemble short-term streamflow forecasting, in: *The Art and Science of Water - 36th*
616 *Hydrology and Water Resources Symposium, HWRS 2015*, 2015.
- 617 Perrin, C., Michel, C., and Andréassian, V.: Improvement of a parsimonious model for streamflow
618 simulation, *J Hydrol (Amst)*, 279, [https://doi.org/10.1016/S0022-1694\(03\)00225-7](https://doi.org/10.1016/S0022-1694(03)00225-7), 2003.
- 619 Peterson, T. J., Saft, M., Peel, M. C., and John, A.: Watersheds may not recover from drought, *Science*
620 (1979), 372, <https://doi.org/10.1126/science.abd5085>, 2021.
- 621 Petty, T. R. and Dhingra, P.: Streamflow Hydrology Estimate Using Machine Learning (SHEM), *J Am*
622 *Water Resour Assoc*, 54, <https://doi.org/10.1111/1752-1688.12555>, 2018.



- 623 Pham, L. T., Luo, L., and Finley, A.: Evaluation of random forests for short-term daily streamflow
624 forecasting in rainfall- And snowmelt-driven watersheds, *Hydrol Earth Syst Sci*, 25,
625 <https://doi.org/10.5194/hess-25-2997-2021>, 2021.
- 626 Pradhan, P., Tingsanchali, T., and Shrestha, S.: Evaluation of Soil and Water Assessment Tool and
627 Artificial Neural Network models for hydrologic simulation in different climatic regions of Asia,
628 *Science of the Total Environment*, 701, <https://doi.org/10.1016/j.scitotenv.2019.134308>, 2020.
- 629 Rahimzad, M., Moghaddam Nia, A., Zolfonoon, H., Soltani, J., Danandeh Mehr, A., and Kwon, H. H.:
630 Performance Comparison of an LSTM-based Deep Learning Model versus Conventional Machine
631 Learning Algorithms for Streamflow Forecasting, *Water Resources Management*, 35,
632 <https://doi.org/10.1007/s11269-021-02937-w>, 2021.
- 633 Reis, G. B., da Silva, D. D., Fernandes Filho, E. I., Moreira, M. C., Veloso, G. V., Fraga, M. de S., and
634 Pinheiro, S. A. R.: Effect of environmental covariable selection in the hydrological modeling using
635 machine learning models to predict daily streamflow, *J Environ Manage*, 290,
636 <https://doi.org/10.1016/j.jenvman.2021.112625>, 2021.
- 637 van Rensch, P., Turner, M., Saft, M., Peel, M. C., Peterson, T. J., Hope, P., and Pepler, A.: The Role of
638 Weather System Changes and Catchment Characteristics in the Rainfall-Runoff Relationship Shift in
639 Victoria, Australia, *Water Resour Res*, 59, <https://doi.org/10.1029/2022wr033692>, 2023.
- 640 Robertson, D. E., Zheng, H., Peña-Arancibia, J. L., Chiew, F. H. S., Aryal, S., Malerba, M., and Wright,
641 N.: How sensitive are catchment runoff estimates to on-farm storages under current and future
642 climates?, *J Hydrol (Amst)*, 626, <https://doi.org/10.1016/j.jhydrol.2023.130185>, 2023.
- 643 Romanowicz, R. J.: Data based mechanistic model for low flows: Implications for the effects of
644 climate change, *J Hydrol (Amst)*, 336, <https://doi.org/10.1016/j.jhydrol.2006.12.015>, 2007.
- 645 Roy, M. H. and Larocque, D.: Robustness of random forests for regression, *J Nonparametr Stat*, 24,
646 <https://doi.org/10.1080/10485252.2012.715161>, 2012.
- 647 Rozos, E., Dimitriadis, P., and Bellos, V.: Machine learning in assessing the performance of
648 hydrological models, *Hydrology*, 9, <https://doi.org/10.3390/hydrology9010005>, 2022.
- 649 Saft, M., Western, A. W., Zhang, L., Peel, M. C., and Potter, N. J.: The influence of multiyear drought
650 on the annual rainfall-runoff relationship: An Australian perspective, *Water Resour Res*, 51,
651 <https://doi.org/10.1002/2014WR015348>, 2015.
- 652 Slater, L. J., Anderson, B., Buechel, M., Dadson, S., Han, S., Harrigan, S., Kelder, T., Kowal, K., Lees, T.,
653 Matthews, T., Murphy, C., and Wilby, R. L.: Nonstationary weather and water extremes: A review of
654 methods for their detection, attribution, and management, [https://doi.org/10.5194/hess-25-3897-](https://doi.org/10.5194/hess-25-3897-2021)
655 2021, 2021.
- 656 Primary Production Landscapes of Victoria - Northwest Victoria:
657 https://vro.agriculture.vic.gov.au/dpi/vro/vrosite.nsf/pages/primary_prod_landscapes_nw_vic, last
658 access: 28 March 2024.
- 659 Stephens, C. M., Marshall, L. A., and Johnson, F. M.: Investigating strategies to improve hydrologic
660 model performance in a changing climate, *J Hydrol (Amst)*, 579,
661 <https://doi.org/10.1016/j.jhydrol.2019.124219>, 2019.
- 662 Szczepanek, R.: Daily Streamflow Forecasting in Mountainous Catchment Using XGBoost, LightGBM
663 and CatBoost, *Hydrology*, 9, <https://doi.org/10.3390/hydrology9120226>, 2022.



- 664 Tongal, H. and Booij, M. J.: Simulation and forecasting of streamflows using machine learning models
665 coupled with base flow separation, *J Hydrol (Amst)*, 564,
666 <https://doi.org/10.1016/j.jhydrol.2018.07.004>, 2018.
- 667 Wallis, A. M., Graymore, M. L. M., and Richards, A. J.: Significance of environment in the assessment
668 of sustainable development: The case for south west Victoria, *Ecological Economics*, 70,
669 <https://doi.org/10.1016/j.ecolecon.2010.11.010>, 2011.
- 670 Wang, K., Band, S. S., Ameri, R., Biyari, M., Hai, T., Hsu, C. C., Hadjouni, M., Elmannai, H., Chau, K. W.,
671 and Mosavi, A.: Performance improvement of machine learning models via wavelet theory in
672 estimating monthly river streamflow, *Engineering Applications of Computational Fluid Mechanics*, 16,
673 <https://doi.org/10.1080/19942060.2022.2119281>, 2022.
- 674 Worland, S. C., Farmer, W. H., and Kiang, J. E.: Improving predictions of hydrological low-flow indices
675 in ungaged basins using machine learning, *Environmental Modelling and Software*, 101,
676 <https://doi.org/10.1016/j.envsoft.2017.12.021>, 2018.
- 677 Yaseen, Z. M., El-shafie, A., Jaafar, O., Afan, H. A., and Sayl, K. N.: Artificial intelligence based models
678 for stream-flow forecasting: 2000-2015, <https://doi.org/10.1016/j.jhydrol.2015.10.038>, 2015.
- 679 Yaseen, Z. M., Jaafar, O., Deo, R. C., Kisi, O., Adamowski, J., Quilty, J., and El-Shafie, A.: Stream-flow
680 forecasting using extreme learning machines: A case study in a semi-arid region in Iraq, *J Hydrol*
681 (Amst), 542, <https://doi.org/10.1016/j.jhydrol.2016.09.035>, 2016.
- 682 Yeturu, K.: Machine learning algorithms, applications, and practices in data science, in: *Handbook of*
683 *Statistics*, vol. 43, <https://doi.org/10.1016/bs.host.2020.01.002>, 2020.
- 684 Zhang, X. S., Amirthanathan, G. E., Bari, M. A., Laugesen, R. M., Shin, D., Kent, D. M., MacDonald, A.
685 M., Turner, M. E., and Tuteja, N. K.: How streamflow has changed across Australia since the 1950s:
686 Evidence from the network of hydrologic reference stations, *Hydrol Earth Syst Sci*, 20,
687 <https://doi.org/10.5194/hess-20-3947-2016>, 2016.
- 688 Zheng, H., Chiew, F. H. S., Post, D. A., Robertson, D. E., Charles, S. P., Grose, M. R., and Potter, N. J.:
689 Projections of future streamflow for Australia informed by CMIP6 and previous generations of global
690 climate models, *J Hydrol (Amst)*, 636, 131286,
691 <https://doi.org/https://doi.org/10.1016/j.jhydrol.2024.131286>, 2024.
- 692